AIMS Mathematics, 9(5): 13410–13438.
DOI: 10.3934/math.2024654
Received: 04 March 2024
Revised: 30 March 2024
Accepted: 03 April 2024
Published: 11 April 2024

https://www.aimspress.com/journal/Math

Research article

A new control scheme for temperature adjustment of electric furnaces using a novel modified electric eel foraging optimizer

Sarah A. Alzakari[1], Davut Izci[2,3,*], Serdar Ekinci[2], Amel Ali Alhussan[1] and Fatma A. Hashim[4,5]

[1] Department of Computer Sciences, College of Computer and Information Sciences, Princess Nourah bint Abdulrahman University, P.O. Box 84428, Riyadh 11671, Saudi Arabia
[2] Department of Computer Engineering, Batman University; Batman 72100, Turkey
[3] Applied Science Research Center, Applied Science Private University, Amman, Jordan
[4] Faculty of Engineering, Helwan University, Egypt
[5] MEU Research Unit, Middle East University, Amman 11831, Jordan

* **Correspondence:** Email: davutizci@gmail.com, davut.izci@batman.edu.tr.

Abstract: In this study, we present a comprehensive framework for enhancing the temperature control of electric furnaces, integrating three novel components: a proportional-integral-derivative controller with a filter (PID-F), a customized objective function, and a modified electric eel foraging optimization (mEEFO) algorithm. The PID-F controller, introduced for the first time in the literature for temperature control of electric furnaces, leverages a filter coefficient to effectively mitigate the kick effect, improving transient and frequency responses. To further optimize the PID-F controller, we employed the mEEFO, a recently proposed metaheuristic inspired by the social predation behaviors of electric eels, with tailored modifications for electric furnace temperature control. The study also introduces a new objective function, based on the modification of the integral of absolute error (IAE) performance index. The proposed framework was evaluated through extensive comparisons with established metaheuristic algorithms, including statistical analysis, Wilcoxon signed-rank test, and time and frequency domain analyses. Comparative assessments with reported methods, such as genetic algorithms and Ziegler–Nichols-based PID controllers, validated the efficacy of the proposed approach, highlighting its transformative impact on electric furnace temperature regulation. The non-ideal conditions such as measurement noise, external disturbance, and saturation at the output of the controller were also evaluated in order to demonstrate the superior performance of the proposed approach from a wider perspective. Furthermore, the robustness of the proposed approach against variations in system parameters was also demonstrated.

Keywords: electric eel foraging optimization; PID-F controller design; metaheuristics; temperature control; electric furnace; non-linear analysis
Mathematics Subject Classification: 90C26, 90C59

1. Introduction

Electric furnaces stand as indispensable components within various industrial processes, playing a pivotal role in the production of metals, alloys, and other critical materials [1]. Their versatility spans applications in metallurgy, glass manufacturing, and chemical industries, contributing significantly to the foundation of modern industrial infrastructure [2–4]. The efficacy of electric furnaces lies in their ability to provide controlled and high-temperature environments essential for the transformation of raw materials into refined products, thereby shaping the backbone of numerous manufacturing sectors [5].

Efficient control of electric furnaces emerges as a paramount concern due to its direct impact on the quality, yield, and energy efficiency of industrial processes. Precise temperature control within these furnaces is imperative to ensure the desired material properties, prevent thermal degradation, and optimize energy consumption. Inaccurate temperature regulation can lead to suboptimal product quality, increased energy costs, and elevated environmental footprints. Therefore, the development of advanced control strategies is of utmost importance [6–8].

The electric furnace temperature-control system is a prevalent real-world second-order system with time delay, widely employed in various industrial production operations [9]. Several control approaches, such as proportional-integral-derivative (PID) control, sliding mode control, predictive control, and internal model control, are utilized for electric furnace temperature control in the industry [10–12]. For instance, a study [13] focused on designing and comparing control strategies for electric furnace temperature regulation, introducing both a linear quadratic regulator (LQR) controller and a PID controller designed using MATLAB. The LQR technique outperformed PID control in achieving better performance for the given electric furnace temperature system. Another work [14] presented a fuzzy logic controller (FLC) for temperature control, particularly in air heater applications. The proposed PDFLC-SSO controller combined a controller structure with fuzzy inference and utilized a trial-and-error method along with a social spider optimization (SSO) algorithm for gain factor tuning. Simulations demonstrated improved performance with PDFLC-SSO, as indicated by a 7.46% integral of time multiplied by absolute error (ITAE) value compared with 9.55% for PDFLC. Addressing temperature control in electric heating furnaces, a study [12] proposed a robust scheme using an adaptive active disturbance rejection control (AADRC) technique with a continuous sliding-mode component. Comparative simulation results showcased the superior robustness and temperature-tracking performance of the proposed method. Additionally, an enhanced flower pollination algorithm (MoFPA) [15] demonstrated superior tracking and regulating responses for electric furnace temperature control compared with PID controllers. Another approach [16] introduced an adaptive lag compensator for electric furnace temperature control, utilizing gorilla troops optimization (GTO) with the balloon effect (BE) (GTO+BE) identifier. The proposed adaptive lag compensator exhibited superior dynamic performance, minimizing overshoot, reducing rise time, and achieving quicker settling time. Furthermore, a fuzzy fractional-order PID control algorithm [17] was proposed for industrial temperature control, dynamically updating gain coefficients based on fractional-order fuzzy rules. This approach proved effective in achieving superior dynamic performance and robustness to

environmental changes. From the related literature, it is evident that the PID controller has been the most preferred structure, similar to other industrial applications due to its simplicity, clear functionality, and applicability [18–25]. It is feasible to encounter more approaches, which are listed in Table 1.

Table 1. Proposed methods in the literature.

Reference	Year	Proposed method
[26]	2010	Improved Smith predictive fuzzy-PID composite control
[27]	2018	Fractional-order predictive functional control
[28]	2024	Adaptive fuzzy-neural control
[29]	2021	Robust state feedback control
[30]	2022	Hybrid intelligent control
[31]	2022	Robust composite control
[32]	2017	Multi-model switching predictive functional control
[33]	2023	Two-degree-of-freedom (2DOF) control
[34]	2020	Implicit proportional-integral-based generalized predictive control

While the PID controller remains a preferred choice, advancing control strategies is crucial for enhancing the overall performance, sustainability, and cost-effectiveness of industrial processes relying on electric furnaces. Hence, this study introduces a novel iteration of the PID controller, termed PID-F (PID with filter) [35], marking the first instance in the literature of its application for temperature control in an electric furnace. The PID-F controller brings a distinct advantage by effectively addressing the kick effect through the incorporation of a filter coefficient into the derivative gain [36]. This addition introduces a new level of adaptability, aiming to improve transient and frequency responses while mitigating the impact of disturbances on the electric furnace temperature-control system.

Choosing an intelligent tuning mechanism holds significant promise for optimizing the PID-F controller, and in this regard, metaheuristic approaches prove crucial due to their problem-free and stochastic structures [37–41]. In alignment with this perspective, this study employs the recently introduced electric eel foraging optimization (EEFO) [42], an advanced optimization technique inspired by the social predation behaviors of electric eels. To enhance the performance and effectiveness of EEFO, specific modifications tailored for electric furnace temperature control are introduced. The modifications include an advanced anti-sine-cosine mechanism [43], which is integrated with control parameters such as randomization control and transfer parameters. These are implemented to tailor the EEFO for more effectively adjusting the parameters of the PID-F controller in the context of electric furnace temperature control, resulting in the modified EEFO (mEEFO) as a more suitable tool for this purpose.

To achieve further improvements, this study introduces a novel objective function, a modification of the integral of absolute error (IAE) performance index [44], for the temperature control of electric furnaces, marking the first instance of such a proposal. Simultaneously, this newly devised objective function takes a prominent role, specifically tailored for the nuanced requirements of electric furnace temperature control. It incorporates essential performance metrics, aligning with the need for swift response, minimal overshoot, and stable settling times. The meticulous design of this objective function aims to navigate the complexities inherent in electric furnace systems, providing a comprehensive metric to assess the effectiveness of the proposed PID-F controller. Therefore, the

advancement of sophisticated control strategies, exemplified by the proposed PID-F controller with a novel modified objective function and the mEEFO algorithm, carries profound significance in elevating the performance, sustainability, and cost-effectiveness of industrial processes reliant on electric furnaces.

In summary, this study amalgamates three groundbreaking elements—the PID-F controller, the customized objective function, and the mEEFO algorithm—creating a unified framework for electric furnace temperature control. Through extensive assessments and comparisons with established metaheuristic algorithms (original EEFO [42], arithmetic optimization algorithm [45], whale optimization algorithm [46], Harris hawks optimization [47], and gravitational search algorithm [48]), we illustrate the transformative impact of this comprehensive approach by statistical analysis, Wilcoxon signed-rank test, convergence behavior, and time and frequency domain analyses. Additionally, a thorough comparison between the proposed mEEFO and established methods, including genetic algorithm [49], Ziegler–Nichols [50], Cohen–Coon [50], and direct synthesis [50] based PID controllers, serves to validate the effectiveness of the proposed approach, pushing the boundaries of achievable performance in electric furnace temperature regulation. The superiority of the proposed approach is ultimately confirmed through various quality indicators.

2. Electric eel foraging optimization

Electric eels, native to South America, serve as the inspiration for electric eel foraging optimization (EEFO) due to their extraordinary predatory abilities [42]. The EEFO integrates the social predation behaviors of electric eels, encompassing interactions, resting, migration, and hunting [51]. The mathematical representations of the foraging behaviors are elucidated as follows.

2.1. Interacting

Inspired by how eels interact during social predation, EEFO employs a cooperative approach where each electric eel represents a candidate solution. In each step, the best candidate solution serves as the intended prey. This interaction phase mimics global exploration, where each eel collaboratively engages with others based on their positions. Specifically:

- Eels engage with a partner randomly selected from the entire population, adjusting their positions based on the difference between the chosen eel and the population center.
- Eels additionally interact with randomly selected partners within the population, modifying their positions by evaluating the disparity between a randomly selected eel and a position generated randomly within the search space.

Interactions involve a churn, representing random movements in various directions. The churn is modeled by the following mathematical representation.

$$C = n_1 \times B, \tag{1}$$

where $n_1 \sim N(0,1)$ and $B = [b_1, b_2, \ldots b_k, \ldots b_d]$. In here, $b(k) = 1$ for $k = g$ and $b(k) = 0$ for otherwise. The term g is determined as $g = randperm(d)$. The interacting behavior is described as:

$$\begin{cases} \begin{cases} v_i(t+1) = x_j(t) + C \times \left(\bar{x}(t) - x_i(t)\right), p_1 > 0.5 \\ v_i(t+1) = x_j(t) + C \times \left(x_r(t) - x_i(t)\right), p_1 \le 0.5 \end{cases} & fit(x_j(t)) < fit(x_i(t)) \\ \begin{cases} v_i(t+1) = x_i(t) + C \times \left(\bar{x}(t) - x_j(t)\right), p_2 > 0.5 \\ v_i(t+1) = x_i(t) + C \times \left(x_r(t) - x_j(t)\right), p_2 \le 0.5 \end{cases} & fit(x_j(t)) \ge fit(x_i(t)) \end{cases}. \tag{2}$$

In here, $x_r = Low + r \times (Up - Low)$, p_1 and p_2 represent random numbers selected from the interval (0, 1). The fitness of the candidate position for the ith electric eel is represented by $fit(x_i)$, where x_j signifies the position of an eel selected randomly from the current population, with $j \neq i$. The variable r corresponds to a random vector within the range (0, 1), while Low and Up represent the lower and upper boundaries, respectively. Besides, $\bar{x}(t)$ is given as:

$$\bar{x}(t) = \frac{1}{n}\sum_{i=1}^{n} x_i(t), \tag{3}$$

where n represents the population size. As defined by Eq (3), the interacting behavior facilitates electric eels to transition to various positions in the search space, significantly contributing to the exploration of the entire search space in the EEFO algorithm.

2.2. Resting

In the EEFO algorithm, it is essential to define a resting area prior to the execution of resting behavior by electric eels. To enhance the effectiveness of the search process, a designated resting area is defined within the portion where one specific dimension of an electric eel's position vector coincides with the main diagonal of the search space. Establishing a resting area entails the normalization of both the search space and the eel's position, ranging from 0 to 1. Subsequently, a randomly chosen dimension from the eel's position is projected onto the main diagonal of the normalized search space, determining the central point of the eel's resting area. The manifestation of the resting behavior is expressed as:

$$v_i(t+1) = R_i(t+1) + n_2 \times (R_i(t+1) - round(rand) \times x_i(t)), \tag{4}$$

where $n_2 \sim N(0,1)$ and R_i is the resting position.

2.3. Hunting

When electric eels locate prey, their hunting strategy involves more than just swarming. Instead, they exhibit cooperative behavior by forming a large circular arrangement to encircle the prey. During this process, they engage in constant communication and collaboration with fellow eels, achieved through low electric organ discharges. As the interaction among eels intensifies, the size of the electrified circle diminishes. Eventually, the eels guide the shoal of fish from deeper waters to shallower areas, making them more accessible as prey. In line with this behavior, the electrified circle serves as the designated hunting area. At this point, the prey begins to maneuver within the hunting area, making sudden and successive movements to various positions due to fear. The hunting behavior displayed by eels, characterized by their curling movement, can be explained as follows:

$$v_i(t+1) = H_{prey}(t+1) + \eta \times (H_{prey}(t+1) - round(rand) \times x_i(t)), \quad (5)$$

where η is the curling factor [42] and H_{prey} the new position of the prey concerning its previous position within the hunting area.

2.4. Migrating

When electric eels locate prey, their tendency is to transition from the resting area to the hunting area. To represent this migratory behavior mathematically, the following equation is employed:

$$v_i(t+1) = -r_5 \times R_i(t+1) + r_6 \times (H_r(t+1) - L \times \big(H_r(t+1) - x_i(t)\big). \quad (6)$$

Here, H_r represents any position within the hunting area, while r_5 and r_6 are random numbers within the range (0,1). The Levy flight function, denoted as L, is incorporated into the exploitation phase of EEFO to prevent entrapment in local optima.

2.5. Transition from exploration to exploitation

In EEFO, the exploration and exploitation transitions crucially depend on an energy factor, optimizing the algorithm's performance [52,53]. The eel's energy factor value serves as the determinant for selecting between exploration and exploitation, and it is formally defined as:

$$E(t) = 4 \times \sin\,(1 - \frac{t}{T}) \times ln\frac{1}{r_7}, \quad (7)$$

where r_7 is a random number within (0,1).

3. Modified electric eel foraging optimization

Traditional metaheuristic algorithms may fail to achieve suboptimal values and suffer from slow and premature convergence rates. Accordingly, an advanced anti-sine-cosine mechanism is introduced and integrated with control parameters like randomization control and transfer parameters.

3.1. Linear transfer function

The linear transfer function (LTF) is a proposed control parameter to achieve the balance between exploration-exploitation phases and guarantee a linear transfer from exploration to exploitation gradually in appreciate time. It is given as follows:

$$LTF = \left(1 - \frac{t}{T}\right). \quad (8)$$

3.2. Randomization operator

The right amount of randomization in each phase of the metaheuristic algorithm is one of the guarantees of success of this algorithm. In mEEFO, we integrated the control parameters in the update

equation with the randomization operator (RO). RO generates a randomization number with different signs to change the arrow of the search agent in a different direction. This avoids stagnation at the local optimum RO given by:

$$RO = 2 \times rand - 1, \tag{9}$$

where rand is a random number [0,1].

3.3. Advanced anti-sine-cosine

This section proposes EEFO with an advanced anti-sine-cosine (AASC) mechanism; the anti-sine-cosine (ASC) mechanism is inspired by the integration between the mutation operators of linear population size reduction adaptive differential evolution (LSHADE) with sine cosine algorithm (SCA). The main idea behind the ASC mechanism is using two mutation strategies injected with arcsine and arccosine functions. Here, the AASC is also injected with two operators, linear transfer function and randomization operator (RO), to achieve information communication between different populations and a good scan of the given workspace. The AASC mechanism is given as follows.

$$\mathrm{X_i(t+1)} = \begin{cases} \mathrm{X_i(t)} + \mathrm{RO} \times LTF \times \arcsin(\mathrm{R}) \times \left[\mathrm{G} \times \left(\mathrm{X_{prey}} - \mathrm{X_i(t)}\right) + \left(\mathrm{X_{r1}(t)} - \mathrm{X_{r2}(t)}\right)\right] & \mathrm{l} < 0.5, \\ \mathrm{X_i(t)} + \mathrm{RO} \times LTF \times \arccos(\mathrm{R}) \times \left[\mathrm{G} \times \left(\mathrm{X_{prey}} - \mathrm{X_i(t)}\right) + \left(\mathrm{X_{r1}(t)} - \mathrm{X_{r2}(t)}\right)\right] & \text{otherwise.} \end{cases} \tag{10}$$

The pseudocode of the proposed mEEFO is given in Algorithm 1.

4. Mathematical modeling of electric furnace temperature-control system

The components of the temperature control system for an electric furnace, as outlined in [50], consist of the electric furnace itself, a controller, and a thermocouple. Figure 1 illustrates the configuration where the controller is employed to regulate the temperature within the electric furnace. In this way, the real-time temperature is detected, and the control algorithm adjusts the power demand of the furnace accordingly.

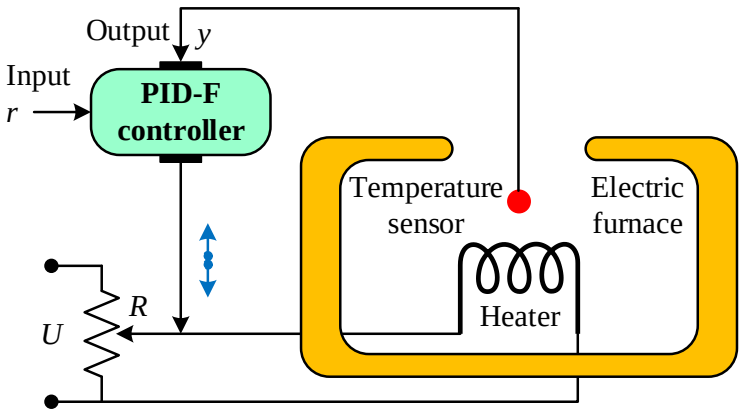

Figure 1. Block diagram of electric furnace temperature control system.

Algorithm 1. Pseudocode of the proposed mEEFO.

1) Initialize EEFO parameters $n,\ T$.
2) Initialize the positions of candidate solutions randomly. $X_i: i = 1, \ldots, n$.
3) While (t <T) do
4) Update LTF
5) Calculate the fitness values (Fit_i) of the candidate solutions (X_i).
6) Find the optimal solution so far X_{prey}.
7) For (i = 1 to N) do
    a) Calculate E.
    b) If $E > 1$
        i) Perform the interacting behavior.
        ii) Evaluate the fitness Fit_i
    c) Else
        i) If $rand < 1/3$
            1) Determining the resting region.
            2) Perform the resting behavior.
            3) Evaluate the fitness Fit_i
        ii) Else If $rand > 2/3$
            1. Perform the migrating behavior.
        iii) Else
            1. Determining the hunting region.
            2. Perform hunting behavior.
        iv) End If
    d) End If
    e) Update each eel's position.
8) End For
9) For ($i = 1\ to\ N$) do
    a) Update randomization operator.
    b) Parameters setting for $r1, r2, l, R$ and G.
    c) Update each solution's position.
10) End For
11) Update the best solution found so far X_{prey}.
12) End While
13) Return X_{prey}.

In the related figure, r represents the input voltage, U stands for the output voltage generated by the controller, y corresponds to the output voltage measured by the thermocouple, and R denotes the armature resistance. In order to analyze the temperature control system of the electric furnace, a mathematical model is derived based on the transfer function. The transfer function of the system is represented by $G_p(s)$ and is given by:

$$G_p(s) = \frac{b_0}{a_2 s^2 + a_1 s + a_0} e^{-Ds} = \frac{0.15}{s^2 + 1.1s + 0.2} e^{-1.5s}. \tag{11}$$

To facilitate analysis and simulation, a first order Padé approximation is employed for the

exponential term e^{-Ds} (using $1.5\,s$ time delay), resulting in:

$$e^{-Ds} \cong \frac{2-Ds}{2+Ds}. \tag{12}$$

Substituting this approximation into Eq (11), the transfer function $G_p(s)$ can be expressed in a simplified form:

$$G_p(s) = \frac{-0.1125s+0.15}{0.75s^3+1.825s^2+1.25s+0.2}. \tag{13}$$

To further characterize the system's behavior, the step response of the system without a controller is analyzed, as depicted in Figure 2.

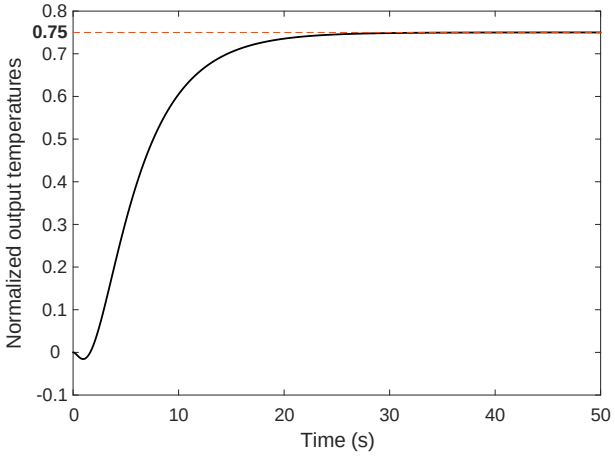

Figure 2. Step response of the system without the controller.

The key performance metrics extracted from the step response are as follows:

- Rise time is $10.2191\ s$.
- Settling time is $19.8657\ s$.
- No (zero) overshoot.

It is important to note that these key performance metrics can be enhanced through the application of novel control methods. Therefore, this study incorporates a novel control mechanism accompanied by an innovative tuning strategy.

5. Proposed novel control method

5.1. The structure of the controller

In this investigation, a novel approach is introduced by employing a proportional-integral-derivative controller with a filter (PID-F) mechanism for the first time in the literature. The performance of the electric furnace system is enhanced through this innovative control strategy. The transfer function of the PID-F controller is defined by Eq (14), wherein the proportional, integral, derivative, and low-pass filter gains are denoted as K_P, K_I, K_D, and N, respectively [35].

$$C_{PID-F}(s) = K_P + \frac{K_I}{s} + K_D \frac{Ns}{s+N}. \tag{14}$$

The PID-F controller offers a distinctive advantage by effectively mitigating the kick effect through the incorporation of a filter coefficient into the derivative gain. Consequently, this modification enhances the immunity of the electric furnace system to noise.

5.2. Objective function

To enhance the temperature control performance of the electric furnace system, the integral of absolute error (IAE), as defined in Eq (15), can be considered a suitable objective function for minimization. The IAE is given by the integral of the absolute difference between the reference signal $r(t)$ and the system output $y(t)$ [54]:

$$IAE = \int_0^\infty |r(t) - y(t)|dt = \int_0^\infty |e(t)|dt. \tag{15}$$

Here, $e(t)$ represents the error between the input and output signals, expressed as $e(t) = r(t) - y(t)$. In the context of temperature control for the electric furnace system, achieving low or no overshoot with a rapid settling time is desirable. To meet these criteria, a novel cost function F is proposed in this study, as described by Eq (16) [44]:

$$F = \rho \times IAE + (1 - \rho) \times T_{set} \tag{16}$$

Here, ρ serves as a balancing coefficient, set to $\rho = 0.70$ for this study, and T_{set} represents the settling time. The proposed cost function combines the integral of absolute error and settling time, reflecting the importance of minimizing overshoot while achieving a swift settling response. For this study, the parameter limitations are established as follows:

- $1 \leq K_P \leq 4$
- $0 \leq K_I \leq 2$
- $3 \leq K_D \leq 7$
- $10 \leq N \leq 500$

These constraints provide a framework for parameter tuning, ensuring the optimization of the temperature control system for the electric furnace.

5.3. Implementation of proposed algorithm

In the pursuit of optimizing the temperature control of the electric furnace system, an innovative approach is adopted, leveraging the proposed mEEFO. This sophisticated algorithm aims to minimize the newly introduced F objective function, thereby facilitating the identification of optimal parameters for the PID-F controller. Figure 3 illustrates the structured integration of the PID-F-controlled system tuned by the mEEFO. This configuration embodies the synergy between the PID-F controller and the mEEFO algorithm, showcasing their collaborative role in refining the control parameters for the electric furnace system. Through this innovative implementation, the study endeavors to establish a robust and efficient temperature-control strategy for the electric furnace system, capitalizing on the synergistic capabilities of the mEEFO algorithm and the PID-F controller.

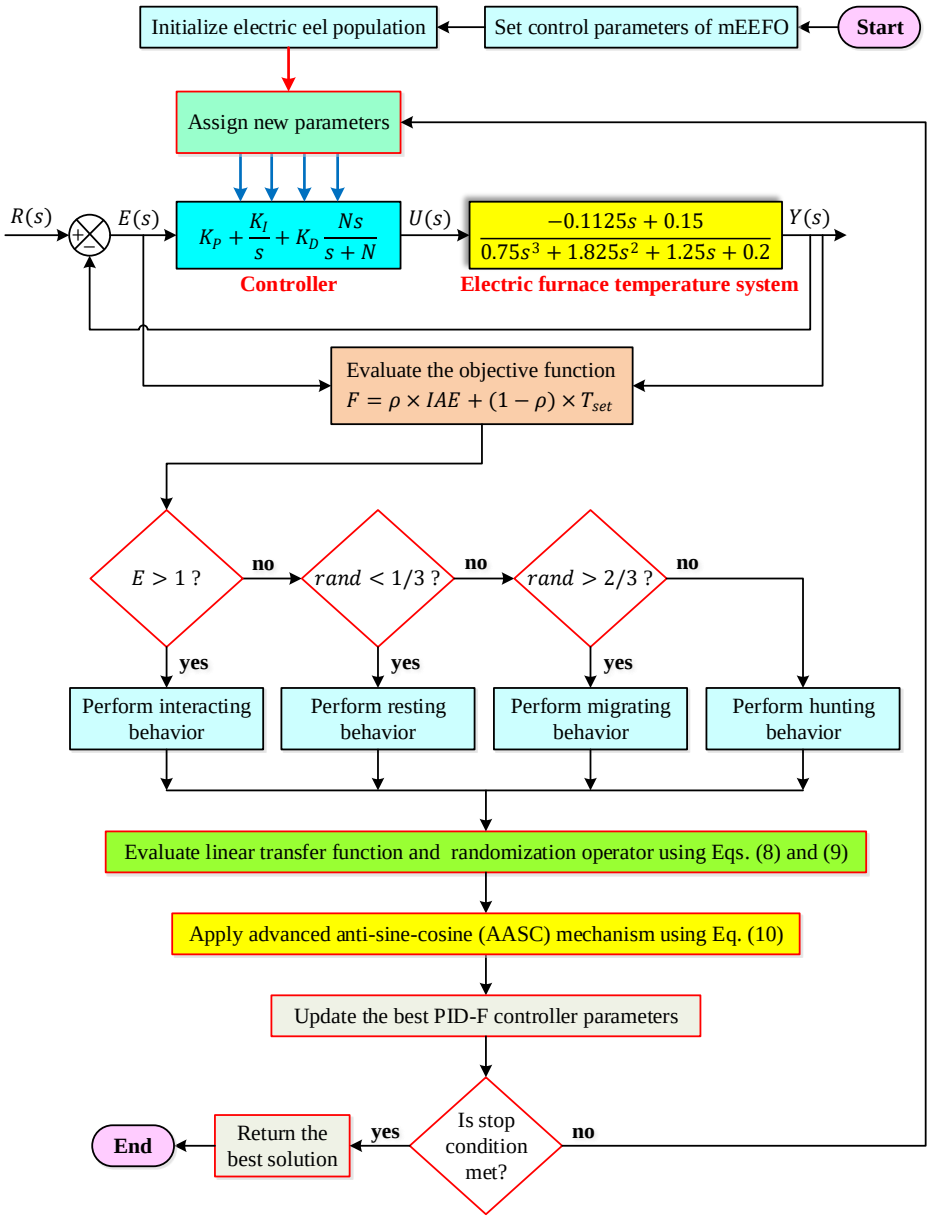

Figure 3. Structure of PID-F-controlled system tuned by mEEFO.

6. Simulation results and discussion

6.1. Developed MATLAB m-file and Simulink model

To facilitate the exploration and validation of the proposed temperature-control strategy for the electric furnace system, a MATLAB-based Simulink model has been developed. This comprehensive model encapsulates the dynamics of the system, integrating the PID-F controller tuned by the mEEFO. The core functionalities of the model are encapsulated within a MATLAB m-file (as shown in Algorithm 2), designed to interface with Simulink for simulation and analysis. This m-file encompasses the implementation of the mEEFO, the PID-F controller, and the dynamics of the electric furnace system. It allows the systematic evaluation of the proposed control strategy.

Algorithm 2. MATLAB codes for mEEFO-based electric furnace temperature-control system.

```
% Open-loop system response
s=tf('s');
G1=0.15/(s^2+1.1*s+0.2); G2=(1-0.75*s)/(1+0.75*s);
G=G1*G2; % step(G), stepinfo(G)
t=0:0.01:50; y_no=step(G, t); stepinfo(y_no, t)
plot(t, y_no, t, 1+t*0)
xlabel('Time (s)'); ylabel('Normalized output temperatures')
% mEEFO-PIDF design
Kp=3.2995; Ki=0.6156; Kd=4.4621; N=368.4193; % Optimized parameters of mEEFO
s=tf('s');
C=Kp+Ki/s+Kd*N*s/(s+N); % PID-F controller
T_meefo_open=G*C; T_meefo=feedback(G*C,1);
t=0:0.01:50; y_meefo=step(T_meefo, t); S=stepinfo(y_meefo, t, 1)
sim(temp_cont_sim') % Developed Simulink model
IAE=J_iae.signals.values(end)
ZLG=(1-exp(-1))*S.Overshoot*0.01+exp(-1)*(S.SettlingTime-S.RiseTime)
Fit=0.70*J_iae.signals.values(end)+0.30*S.SettlingTime % Fitness function evaluation
bode(T_meefo_open); [Gm,Pm] = margin(T_meefo_open);
bandwidth(T_meefo), GmdB=20*log10(Gm), Pm
```

Figure 4 visually presents the architecture of the Simulink model, encapsulating the interconnected components, feedback loops, and the PID-F-controlled system tuned by the mEEFO. This Simulink model becomes a crucial tool for experimentation, enabling the investigation of the proposed control strategy's efficacy under diverse scenarios and conditions.

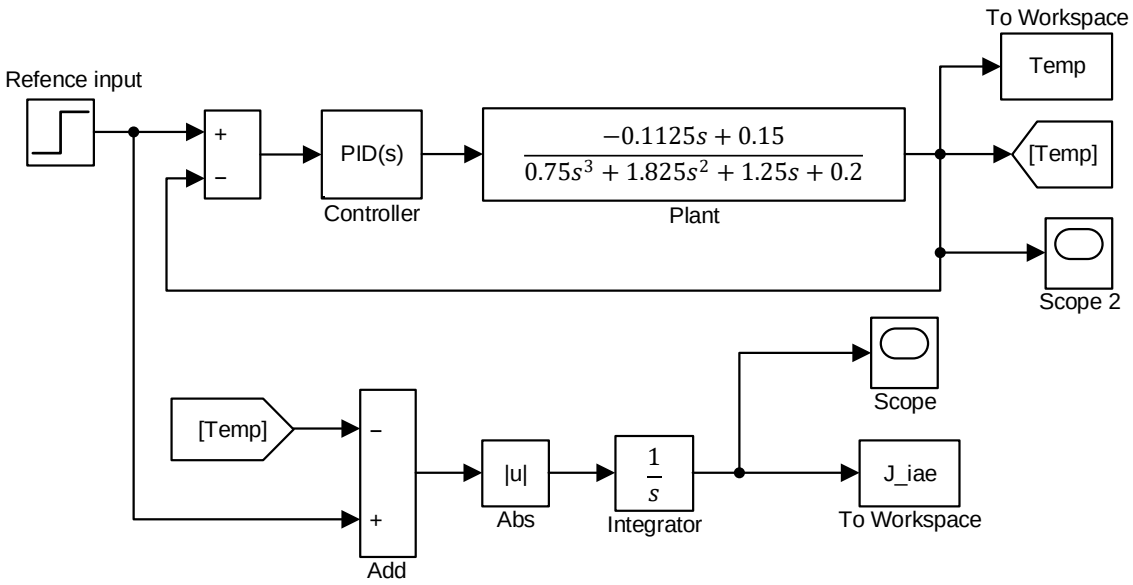

Figure 4. Simulink model for temperature control of electric furnace system.

6.2. Compared metaheuristic algorithms

To comprehensively assess the performance of the proposed mEEFO, a comparative study is conducted, involving well-established metaheuristic algorithms. In addition to the original electric eel foraging optimization (EEFO) [42], this evaluation incorporates recent and highly effective algorithms, including the arithmetic optimization algorithm (AOA) [45], whale optimization algorithm (WOA) [46], Harris hawks optimization (HHO) [47], and gravitational search algorithm (GSA) [48]. The selected metaheuristic algorithms (as shown in Table 2) were chosen for their prominence in optimization tasks. These algorithms, each renowned for specific attributes, contribute to a thorough examination of the proposed mEEFO. This comprehensive comparison can provide valuable insights into the relative strengths and weaknesses of the proposed mEEFO against established optimization methods, shedding light on its efficacy in the context of temperature control for the electric furnace system.

Table 2. Parameter settings for all algorithms.

Algorithms	Population size	Maximum iterations	Other control parameters
mEEFO (proposed)	30	50	-
EEFO [42]	30	50	-
AOA [45]	30	50	Sensitive parameter $\alpha = 5$, control parameter $\mu = 0.499$
WOA [46]	30	50	Convergence parameter (a) linearly decreases from 2 to 0
HHO [47]	30	50	Random variable $E_0 \in [-1, 1]$
GSA [48]	30	50	Gravitational constant $G_0 = 100$, decreasing coefficient $a = 20$

6.3. Statistical analysis

To comprehensively evaluate the performance of the metaheuristic algorithms in minimizing the objective function, a detailed statistical analysis was conducted, revealing significant insights into their comparative effectiveness. Figure 5 provides a visual representation of the statistical analysis considering all runs for each algorithm. The results showcase the efficacy of each algorithm in achieving the minimization of the objective function. Notably, the proposed mEEFO demonstrates superior performance, as reflected in its competitive position among the algorithms.

The boxplots provide a comprehensive view of the spread and central tendencies, allowing for a deeper understanding of the algorithms' consistency and robustness in achieving optimal solutions. In Figure 6, the boxplot analysis further elucidates the distribution and variability of the performance results across multiple runs for each algorithm.

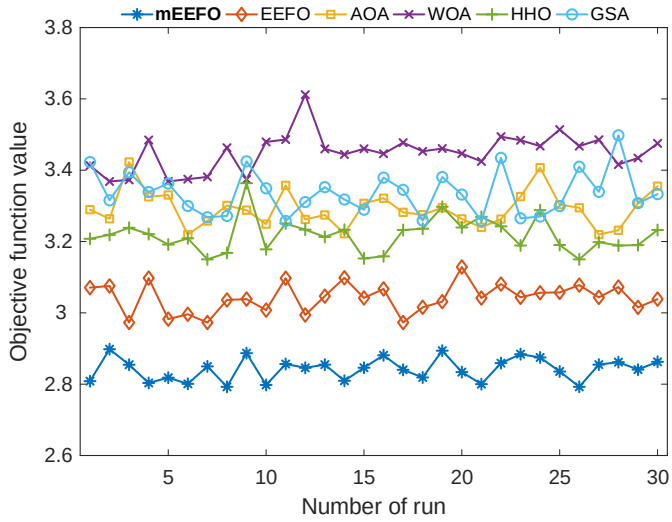

Figure 5. Statistical analysis for the minimization of the objective function considering all runs.

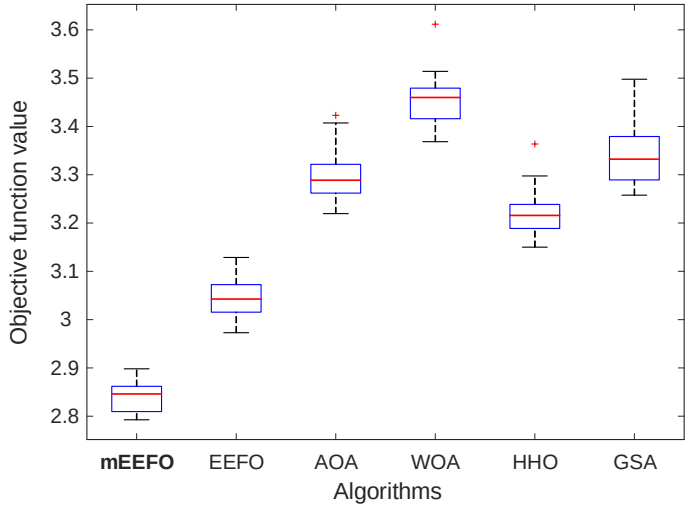

Figure 6. Boxplot analysis.

Table 3 presents a numerical overview of the statistical performance of the algorithms, capturing key metrics such as the best, worst, mean, standard deviation (SD), median, and rank for each algorithm. The values underscore the efficacy of the algorithms in objective function minimization.

Table 3. Numerical presentation of the statistical performance of the algorithms.

Algorithms	Best	Worst	Mean	SD	Median	Rank
mEEFO	2.7926	2.8982	2.8420	0.0318	2.8461	1
EEFO	2.9729	3.1287	3.0424	0.0409	3.0426	2
AOA	3.2195	3.4230	3.2919	0.0501	3.2887	4
WOA	3.3685	3.6117	3.4496	0.0523	3.4600	6
HHO	3.1501	3.3637	3.2177	0.0472	3.2158	3
GSA	3.2577	3.4978	3.3362	0.0612	3.3323	5

The proposed mEEFO achieved the best performance with a minimum objective function value of 2.7926. This indicates that mEEFO consistently found solutions with the lowest objective function values among all algorithms. Examining the standard deviation, mEEFO exhibited the lowest value (0.0318), suggesting a high level of consistency and robustness in achieving optimal solutions. A lower standard deviation implies less variability in performance across multiple runs. The median value for mEEFO (2.8461) is close to the best performance, indicating a stable and reliable performance across various optimization runs. This aligns with the visual representation in Figure 6, where the boxplot shows a tight distribution of results for mEEFO. The rank column reveals that mEEFO secured the top position (Rank 1) among all algorithms. This consistent top ranking indicates the algorithm's superiority in minimizing the objective function compared with the other metaheuristic algorithms considered. Notably, mEEFO outperformed the original EEFO, AOA, WOA, HHO, and GSA in terms of achieving lower objective function values. These results collectively suggest that the proposed mEEFO algorithm demonstrates exceptional efficiency, reliability, and effectiveness in optimizing the temperature control of the electric furnace system. The consistency in achieving superior results across multiple runs underscores the algorithm’s robustness and potential applicability in practical scenarios.

6.4. Wilcoxon test

Table 4 presents the results of the nonparametric Wilcoxon signed-rank test, offering valuable insights into the statistical significance of performance differences between the proposed mEEFO and its competitors. The p-values obtained from the Wilcoxon test for all comparisons between mEEFO and its competitors are remarkably small (1.7344E−06), suggesting highly significant differences in performance. In all comparisons, the p-values are consistent, indicating that mEEFO is statistically superior to EEFO, AOA, WOA, HHO, and GSA. The "Superior" column unequivocally states that mEEFO outperforms the respective competitors in each comparison. The small p-value (1.7344E−06) underscores the high statistical significance of the observed differences. This provides strong evidence to reject the null hypothesis, affirming the superiority of mEEFO. These findings, supported by the Wilcoxon signed-rank test, further reinforce the robust performance and effectiveness of the proposed mEEFO algorithm in comparison to established metaheuristic algorithms. The consistent superiority across multiple comparisons highlights mEEFO as a statistically significant and reliable optimization strategy for the temperature control of the electric furnace system.

Table 4. p-values obtained from nonparametric Wilcoxon signed-rank test.

Proposed	Competitor	p-value	Superior
mEEFO	EEFO	1.7344E−06	mEEFO
mEEFO	AOA	1.7344E−06	mEEFO
mEEFO	WOA	1.7344E−06	mEEFO
mEEFO	HHO	1.7344E−06	mEEFO
mEEFO	GSA	1.7344E−06	mEEFO

6.5. Change of objective function and obtained best controller parameters

In this section, we delve into the convergence behavior of the proposed mEEFO in comparison to other metaheuristic algorithms. Additionally, the obtained best controller parameters and their

corresponding closed-loop transfer functions are presented for a comprehensive understanding of the optimization process. Figure 7 showcases the convergence curves of the objective function for mEEFO, EEFO, AOA, WOA, HHO, and GSA. It is evident from the convergence curves that mEEFO consistently reaches the lowest objective function values compared with the other algorithms, affirming its effectiveness in rapidly converging to optimal solutions.

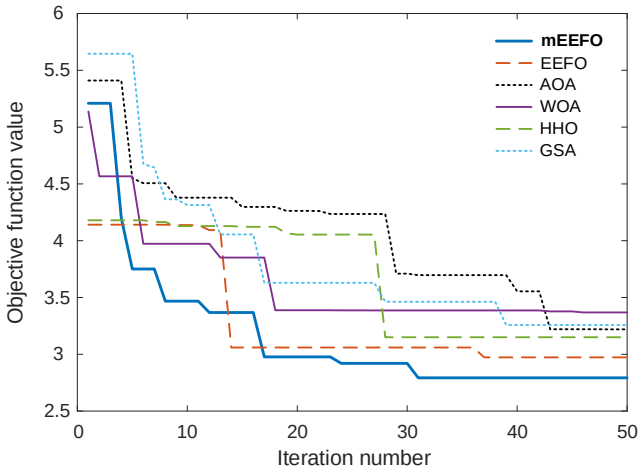

Figure 7. Convergence curves of objective function for mEEFO, EEFO, AOA, WOA, HHO, and GSA.

Table 5 provides a comprehensive overview of the best controller parameters obtained through the optimization process for each algorithm. Additionally, the table includes the respective closed-loop transfer functions, offering insights into the dynamic characteristics of the optimized controllers. These parameters are critical in achieving optimal closed-loop performance for the temperature-control system. The combined analysis of convergence behavior and obtained controller parameters offers a holistic perspective on the efficacy of the optimization algorithms in tailoring controllers for the temperature control of the electric furnace system. The dominance of mEEFO in convergence and parameter optimization underscores its potential for practical implementation in real-world control scenarios.

6.6. Step response analysis

In this section, we delve into the time domain–based performance of different optimization algorithms by analyzing their step responses. The step response is a crucial indicator of the system's performance in terms of stability, speed, and precision. Figure 8 illustrates the step responses of various algorithms, providing valuable insights into their dynamic behavior. Additionally, Figure 9 offers a closer examination of the step responses presented in Figure 8, focusing on key performance indicators such as overshoot (OS), rise time (T_{rise}), and settling time (T_{set}).

Table 5. Obtained best controller parameters and the respective closed-loop transfer functions.

Algorithms	K_P	K_I	K_D	N	Closed-loop transfer function
mEEFO	3.2995	0.6156	4.4621	368.4193	$\frac{-185.3s^3 + 110.3s^2 + 156.9s + 34.02}{0.75s^5 + 278.1s^4 + 488.3s^3 + 571s^2 + 230.6s + 34.02}$
EEFO	3.1365	0.5925	4.1063	482.4784	$\frac{-223.2s^3 + 127.3s^2 + 194.9s + 42.88}{0.75s^5 + 363.7s^4 + 658.5s^3 + 730.6s^2 + 291.4s + 42.88}$
AOA	3.2516	0.5874	4.0930	276.9906	$\frac{-127.9s^3 + 69.16s^2 + 116.9s + 24.41}{0.75s^5 + 209.6s^4 + 378.8s^3 + 415.6s^2 + 172.3s + 24.41}$
WOA	3.3376	0.5802	4.0353	86.5032	$\frac{-39.65s^3 + 20.32s^2 + 37.75s + 7.528}{0.75s^5 + 66.7s^4 + 119.5s^3 + 128.6s^2 + 55.05s + 7.528}$
HHO	3.2920	0.6205	4.3618	247.8975	$\frac{-122s^3 + 70.81s^2 + 105.2s + 23.07}{0.75s^5 + 187.7s^4 + 331.6s^3 + 380.9s^2 + 154.8s + 23.07}$
GSA	3.2147	0.5537	3.8479	364.1738	$\frac{-158s^3 + 78.91s^2 + 153s + 30.25}{0.75s^5 + 275s^4 + 507.9s^3 + 534.3s^2 + 225.8s + 30.25}$

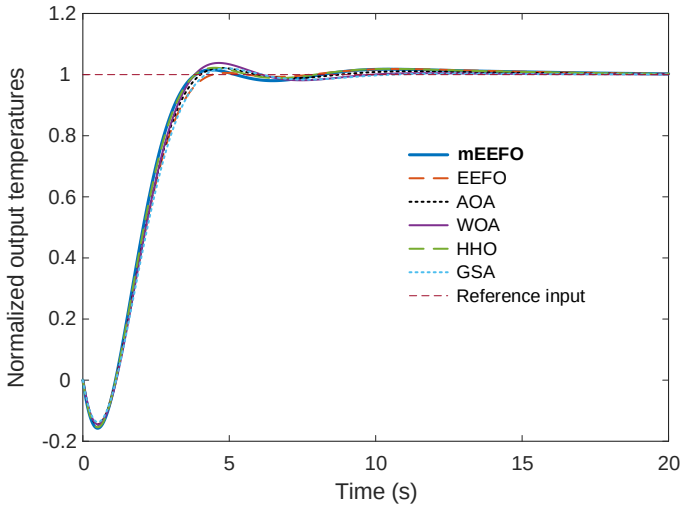

Figure 8. Step responses of different algorithms.

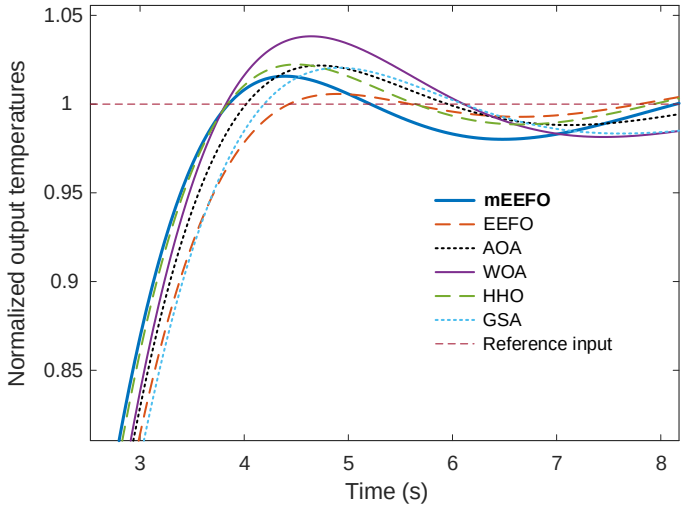

Figure 9. Zoomed-in view of step responses.

Table 6 provides a numerical assessment of the time domain–based performance metrics, offering quantitative values for overshoot, rise time, and settling time for each algorithm. The numerical values in Table 6 demonstrate that mEEFO achieves the lowest overshoot (1.7563%), indicating superior control over transient oscillations compared with other algorithms. mEEFO exhibits the lowest rise time ($1.8078\ s$), signifying a quicker response to changes in the reference signal compared with its counterparts. With a settling time of $3.6176\ s$, mEEFO outperforms other algorithms in achieving stability and precision in a shorter time duration. These results collectively suggest that mEEFO not only excels in the optimization process but also translates to superior dynamic performance in the time domain. The step response analysis, supported by numerical values, further reinforces the efficacy of mEEFO in achieving precise and efficient temperature control for the electric furnace system.

Table 6. Numerical assessment of time domain–based performance.

Algorithms	OS (%)	T_{rise} (s)	T_{set} (s)
mEEFO	1.7563	1.8078	3.6176
EEFO	1.8421	2.0330	4.0212
AOA	2.1749	1.9364	4.9761
WOA	3.8198	1.8674	5.4821
HHO	2.2336	1.8297	4.7739
GSA	2.0468	2.0378	5.0418

6.7. Frequency response analysis

This section focuses on the frequency domain–based performance of various optimization algorithms through the examination of Bode diagrams. Figure 10 visually represents the Bode diagrams for each algorithm, providing insights into their frequency response characteristics. Additionally, Table 7 offers a numerical assessment of key frequency domain parameters, including phase margin (M_{phase}), gain margin (M_{gain}), and bandwidth (W_{band}).

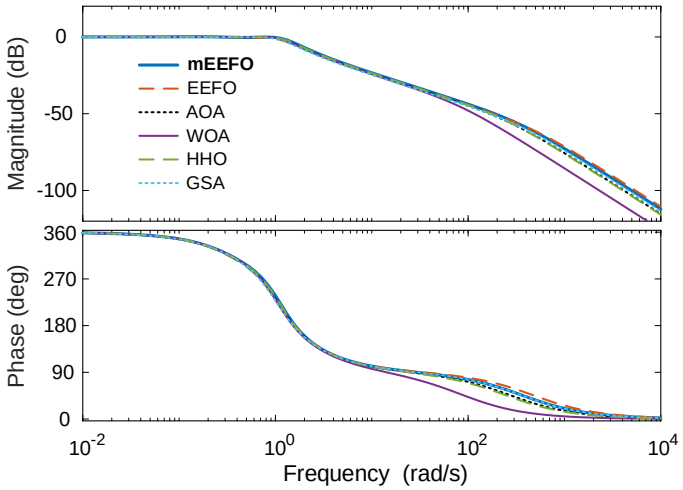

Figure 10. Bode diagrams of the algorithms.

As seen from Table 7, mEEFO exhibits a phase margin of $62.784°$, reflecting a robust stability margin in the frequency domain. This indicates a healthy margin before the system becomes unstable. With a gain margin of $8.3291\ dB$, mEEFO demonstrates a satisfactory buffer against gain variations, contributing to system stability. The bandwidth of 1.4525 rad/s for mEEFO indicates the range of frequencies where the system operates effectively, providing valuable information about the algorithm's responsiveness to input signals. In summary, the frequency response analysis suggests that mEEFO not only excels in the time domain but also exhibits favorable characteristics in the frequency domain. The phase margin, gain margin, and bandwidth values collectively contribute to a comprehensive understanding of the algorithm's stability and performance across different frequencies.

Table 7. Numerical assessment of frequency domain–based performance.

Algorithms	M_{phase} (°)	M_{gain} (dB)	W_{band} (rad/s)
mEEFO	62.7840	8.3291	1.4525
EEFO	63.0627	8.9281	1.3027
AOA	61.7872	8.7470	1.3266
WOA	60.4229	8.5523	1.3379
HHO	62.0265	8.4250	1.4181
GSA	61.7277	9.0409	1.2476

6.8. Comparison with reported methods

In this section, we conduct a comprehensive comparison between the proposed mEEFO and reported methods, including genetic algorithm (GA) [49], Ziegler–Nichols (ZN) [50], Cohen–Coon (CC) [50], and direct synthesis (DS) [50]-based PID controllers. The evaluation encompasses both time-domain and frequency-domain performance metrics to provide a holistic understanding of the comparative effectiveness of these methods.

Figure 11 presents comparative step responses, allowing for a visual assessment of the dynamic behavior of the systems controlled by mEEFO and reported methods. This comparison provides insights into the transient response characteristics, emphasizing overshoot, rise time, and settling time.

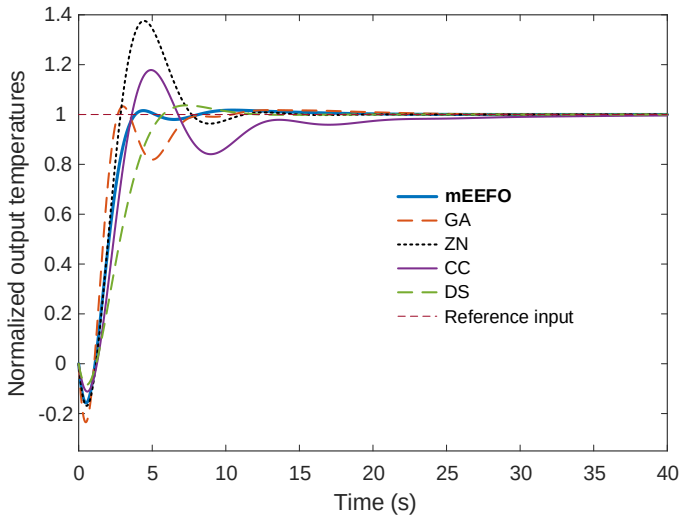

Figure 11. Comparative step responses with reported methods.

Table 8 offers a numerical assessment of the time-domain performance, providing quantitative values for overshoot, rise time, and settling time for mEEFO and reported methods. As seen from this table, mEEFO exhibits the lowest overshoot among all methods, indicating superior control over transient oscillations. It achieves a competitive rise time, emphasizing its responsiveness to changes in the reference signal. mEEFO also outperforms other methods in settling time, achieving stability and precision in a shorter duration.

Table 8. Comparative time domain–based performance assessment.

Algorithms	OS (%)	T_{rise} (s)	T_{set} (s)
mEEFO	1.7563	1.8078	3.6176
GA	3.2725	1.1378	7.3185
ZN	37.5675	1.2840	10.1386
CC	17.8485	1.7853	21.4023
DS	3.6937	3.0806	9.3605

Figure 12 illustrates comparative Bode diagrams, providing insights into the frequency response characteristics of mEEFO and reported methods. This analysis focuses on phase margin, gain margin, and bandwidth, offering a detailed view of stability and performance in the frequency domain.

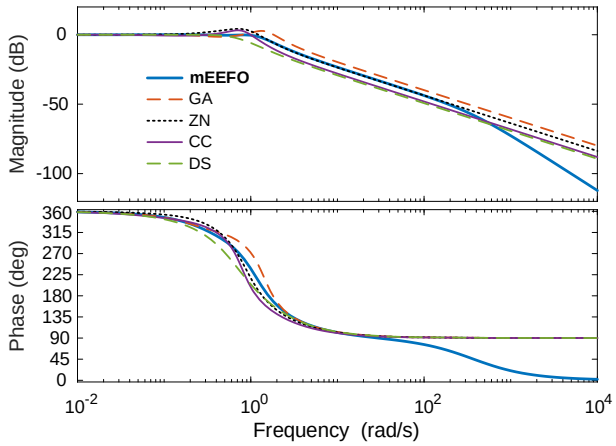

Figure 12. Comparative Bode diagrams with reported methods.

Table 9 offers numerical values for phase margin, gain margin, and bandwidth, facilitating a quantitative assessment of the frequency-domain performance for mEEFO and reported methods. From this table, it can be seen that mEEFO and DS demonstrate competitive phase margins, indicating robust stability in the frequency domain. mEEFO and DS exhibit favorable gain margins, providing a buffer against gain variations for stable system operation. mEEFO achieves a competitive bandwidth, showcasing its effectiveness in responding to a range of input frequencies. In summary, the comprehensive comparison with reported methods highlights the superior performance of mEEFO, both in the time and frequency domains. The visual representation and numerical assessment underscore the efficacy of mEEFO in achieving precise and stable control for the electric furnace system when compared with established control methods.

Table 9. Comparative frequency domain–based performance assessment.

Algorithms	M_{phase} (°)	M_{gain} (dB)	W_{band} (rad/s)
mEEFO	62.7840	8.3291	1.4525
GA	68.9974	5.8858	2.2322
ZN	36.9753	6.8084	1.4966
CC	45.8826	7.5116	1.1753
DS	61.1560	11.7940	0.7403

6.9. Performance evaluation via quality indicator

For this study, we have proposed a new F objective function, as outlined in section 5.2, which is based on a modified IAE quality indicator. This has been designated to achieve low or no overshoot with a rapid settling time for temperature control of the electric furnace system. To further demonstrate the efficacy of the proposed approach, the actual IAE performance metric [54] has also been used as a quality indicator. Besides, a well-known time-domain criteria-based performance metric known as Zwee-Lee-Gaing (ZLG) [55,56] has also been adopted for further assessment. The structure of the IAE quality indicator has already been expressed in section 5.2. The ZLG quality indicator is given by [57]:

$$ZLG = (1-\delta) \times \left(\frac{\%OS}{100} + E_{ss}\right) + \delta \times (T_{set} - T_{rise}), \tag{17}$$

where $\delta = e^{-1} = 0.3679$ serves as a balancing factor and E_{ss} is steady state error.

The comparative values of the IAE quality indicator obtained via different approaches are presented in Figure 13. Figure 14, on the other hand, displays the comparative values of ZLG quality indicator obtained via different approaches. As seen from those illustrations, the proposed mEEFO reaches the smallest values both for IAE (2.4390) and ZLG (0.6769) quality indicators, making it the more efficient approach even with different performance indices.

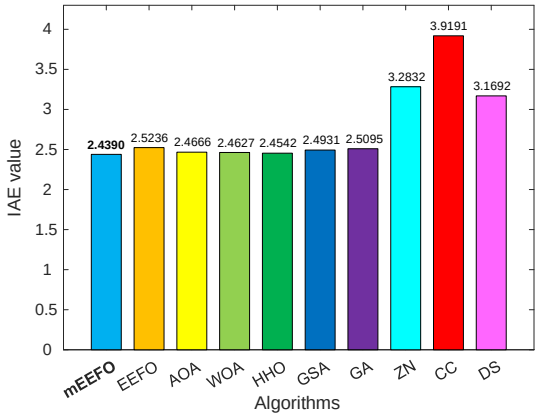

Figure 13. Comparative values of IAE quality indicator obtained via different approaches.

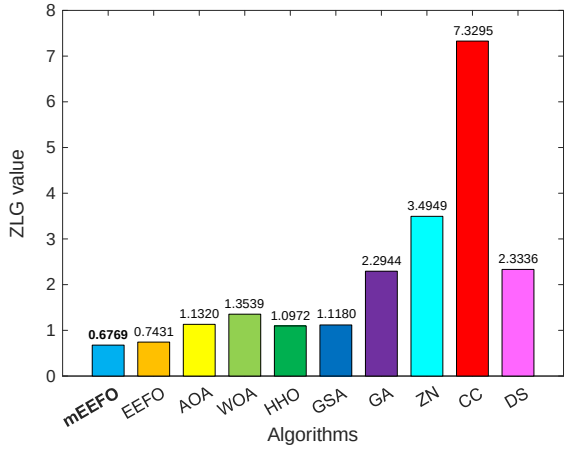

Figure 14. Comparative values of ZLG quality indicator obtained via different approaches.

6.10. *Robustness validation of proposed controller*

The robustness of a control system is a desirable feature that gauges its capability to endure uncertainties and disturbances across its parameters, inputs, outputs, and environment [58,59]. Considering this important feature, we have performed a robustness analysis by considering the scenarios presented in Table 10. As seen from the numerical results provided in the respective table, the proposed mEEFO has greater capability in terms of handling the parametric variations, which makes it superior in terms of robustness.

Table 10. The robustness performance of PID-F-controlled system tuned by mEEFO and EEFO algorithms.

Scenario	Algorithms	OS (%)	T_{rise} (s)	T_{set} (s)
$a_2 = 1.16,\ a_1 = 1.075,$	mEEFO	1.3119	2.7277	5.2390
$a_0 = 0.195,\ b_0 = 0.12$	EEFO	1.5061	2.9867	5.6119
$a_2 = 0.85,\ a_1 = 1.125,$	mEEFO	0.8669	1.5984	7.4600
$a_0 = 0.22,\ b_0 = 0.16$	EEFO	0.9470	1.8676	7.5230

6.11. *Performance evaluation for non-ideal conditions*

To further demonstrate the superior efficacy of the proposed approach, a more realistic model for the temperature control of an electric furnace system has also been considered in this study. In this regard, more real conditions, such as measurement noise as a disturbance source, external disturbance, and the saturation at the input of the system as a non-linear effect in the electric furnace temperature system, were considered. The respective system with such non-ideal conditions is illustrated in Figure 15.

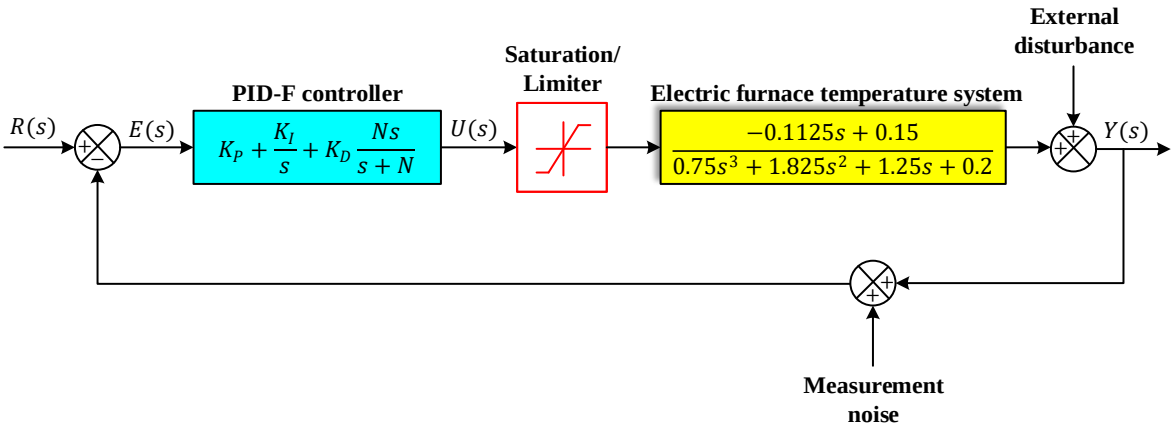

Figure 15. A more realistic model for temperature control in an electric furnace system.

With regards to measurement noise, white Gaussian noises with a signal-to-noise ratio (SNR) of 20 dB were considered. The normalized output temperature changes considering ideal and non-ideal conditions are displayed in Figure 16. As can be observed from this figure, the proposed method is quite capable of handling the non-linear effects by quickly recovering the desired output.

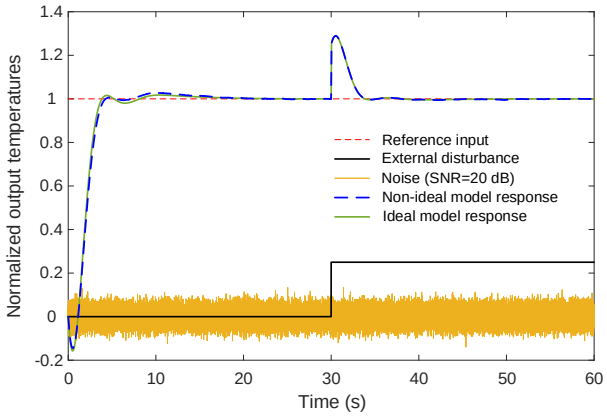

Figure 16. Step responses of mEEFO-tuned system with ideal and non-ideal conditions.

7. Conclusions

This study has introduced a comprehensive framework for the temperature control of electric furnaces, combining innovative elements such as the PID-F controller, a novel modified objective function, and the mEEFO algorithm. Through extensive evaluations and comparisons with established metaheuristic algorithms including the original EEFO, arithmetic optimization algorithm, whale optimization algorithm, Harris hawks optimization, and gravitational search algorithm, the proposed approach demonstrates transformative impact across various analyses. The structured abstract reveals the effectiveness of the holistic approach in terms of statistical analysis, Wilcoxon signed-rank test, convergence behavior, time and frequency domain analyses, as well as comprehensive comparisons with reported methods like genetic algorithm, Ziegler–Nichols, Cohen–Coon, and direct synthesis–based PID controllers. The superiority of the proposed approach is highlighted through various quality indicators, marking a significant advancement in electric furnace temperature regulation. In light of the above discussion, the significant contributions of this work can briefly be listed as follows.

- The mEEFO algorithm was developed by integrating effective operators into the current EEFO algorithm.
- A mEEFO-based PID-F controller for the electric furnace temperature control system was proposed for the first time.
- Detailed comparisons were provided with significant control methods reported in the literature and various metaheuristic optimization methods with different sources of inspiration.
- The effectiveness and potential of the proposed control method under non-ideal conditions were validated through statistical analyses, Wilcoxon tests, convergence curves, step response, frequency response, and robustness analyses.

As a pathway for future research, several promising directions emerge from this study. First, exploring the adaptability and performance of the proposed framework in real-world industrial settings would provide valuable insights into its practical applicability. Additionally, investigating the impact of varying environmental conditions and system uncertainties on the proposed approach could enhance its robustness. Further refinement and optimization of the mEEFO algorithm and exploration of alternative objective functions could lead to even more sophisticated control strategies. Collaborative efforts between control engineers and industry practitioners may facilitate the integration of this framework into industrial automation systems. Finally, extending the study to encompass multi-

variable systems and addressing the challenges associated with non-linearities and external disturbances would contribute to a more comprehensive understanding of the proposed framework's capabilities in complex industrial scenarios.

Use of AI tools declaration

The authors declare they have not used Artificial Intelligence (AI) tools in the creation of this article.

Acknowledgments

The authors would like to express their gratitude to Princess Nourah bint Abdulrahman University Researchers Supporting Project number (PNURSP2024R716), Princess Nourah bint Abdulrahman University, Riyadh, Saudi Arabia.

Funding

This research was funded by Princess Nourah bint Abdulrahman University Researchers Supporting Project number (PNURSP2024R716), Princess Nourah bint Abdulrahman University, Riyadh, Saudi Arabia.

Conflict of interest

The authors declare that they have no conflict of interest.

References

1. P. L. V. Héroult, Recent developments in the electric steel furnace, *Ind. Eng. Chem.*, **5** (1913), 47–49. https://doi.org/10.1021/ie50049a020
2. J. C. Tudon-Martinez, J. de-J. Lozoya-Santos, A. Cantu-Perez, A. Cardenas-Romero, Advanced temperature control applied on an industrial box furnace, *J. Therm. Sci. Eng. Appl.*, **14** (2022), 061001.
3. N. Wang, Z. X. Liu, C. Ding, J. Zhang, G. Sui, H. Jia, et al., High efficiency thermoelectric temperature control system with improved proportional integral differential algorithm using energy feedback technique, *IEEE T. Ind. Electron.*, **69** (2022), 5225–5234. https://doi.org/10.1109/TIE.2021.3082462
4. J. Tang, H. Ni, R. Peng, N. Wang, L. Zuo, A review on energy conversion using hybrid photovoltaic and thermoelectric systems, *J. Power Sources*, **562** (2023), 232785. https://doi.org/10.1016/j.jpowsour.2023.232785
5. H. Etchells, Application of electric furnace methods to industrial processes, *Trans. Faraday Soc.*, **14** (1919), 71–78.
6. M. M. Hussein, S. Alkhalaf, T. H. Mohamed, D. S. Osheba, M. Ahmed, A. Hemeida, et al., Modern temperature control of electric furnace in industrial applications based on modified optimization technique, *Energies*, **15** (2022), 8474. https://doi.org/10.3390/en15228474

7. E. Grassi, K. Tsakalis, PID controller tuning by frequency loop-shaping: application to diffusion furnace temperature control, *IEEE T. Contr. Syst. Technol.*, **8** (2000), 842–847. https://doi.org/10.1109/87.865857
8. D. Ajorloo, M. Nazari, M. Nazari, N. Sepehry, A. Mohammadzadeh, Mathematical modeling and designing an optimized fuzzy temperature controller for a vacuum box electric furnace: Numerical and experimental study, *T. I. Meas. Control*, **45** (2023), 1193–1212. https://doi.org/10.1177/01423312221124017
9. B. G. Liptak, *Instrument engineers' handbook, volume two: Process control and optimization*, CRC Press, 2005. https://doi.org/10.1201/9781315219028
10. X. Chen, Temperature control in electric furnaces: Methods, applications, and challenges, *J. Phys. Conf. Ser.*, **2649** (2023), 012032. https://doi.org/10.1088/1742-6596/2649/1/012032
11. Y. Wang, PID Temperature control, In: *Conveyor belt furnace thermal processing*, Springer, Cham, 2018, 63–76. https://doi.org/10.1007/978-3-319-69730-7_9
12. K. Rsetam, M. Al-Rawi, Z. Cao, Robust adaptive active disturbance rejection control of an electric furnace using additional continuous sliding mode component, *ISA T.*, **130** (2022), 152–162. https://doi.org/10.1016/j.isatra.2022.03.024
13. D. Rawat, K. Bansal, A. K. Pandey, LQR and PID design technique for an electric furnace temperature control system, In: *Proceeding of International Conference on Intelligent Communication, Control and Devices*, 2017, 561–567. Singapore: Springer,. https://doi.org/10.1007/978-981-10-1708-7_64
14. T. Ghanim, A. R. Ajel, A. j. Humaidi, Optimal fuzzy logic control for temperature control based on social spider optimization, *IOP Conf. Ser. Mater. Sci. Eng.*, **745** (2020), 012099. https://doi.org/10.1088/1757-899X/745/1/012099
15. N. Pringsakul, D. Puangdownreong, Mofpa-based pida controller design optimization for electric furnace temperature control system, *Int. J. Innov. Comput. Inform. Control*, **16** (2020), 1863–1876.
16. M. R. Moussa, Temperature control of electric furnace using adaptive lag compensator based on improved gorilla troops optimization: Towards energy efficiency, *Aswan Univ. J. Sci. Technol.*, **3** (2023), 13–29.
17. L. Liu, D. Xue, S. Zhang, General type industrial temperature system control based on fuzzy fractional-order PID controller, *Complex Intell. Syst.*, **9** (2023), 2585–2597. https://doi.org/10.1007/s40747-021-00431-9
18. A. E. Kayabekir, G. Bekdaş, S. M. Nigdeli, Z. W. Geemet, Optimum design of PID controlled active tuned mass damper via modified harmony search, *Appl. Sci.*, **10** (2020), 2976. https://doi.org/10.3390/app10082976
19. S. Ulusoy, S. M. Nigdeli, G. Bekdaş, Novel metaheuristic-based tuning of PID controllers for seismic structures and verification of robustness, *J. Build. Eng.*, **33** (2021), 101647. https://doi.org/10.1016/j.jobe.2020.101647
20. E. Kose, Optimal control of AVR system with tree seed algorithm-based PID controller, *IEEE Access*, **8** (2020), 89457–89467. https://doi.org/10.1109/ACCESS.2020.2993628
21. R. Alayi, F. Zishan, S. R. Seyednouri, R. Kumaret, M. H. Ahmadi, M. Sharifpur, Optimal load frequency control of island microgrids via a PID controller in the presence of wind turbine and PV, *Sustainability*, **13** (2021), 10728. https://doi.org/10.3390/su131910728

22. S. Ekinci, D. Izci, M. R. Al Nasar, L. Abualigah, Logarithmic spiral search based arithmetic optimization algorithm with selective mechanism and its application to functional electrical stimulation system control, *Soft Comput.*, **26** (2022), 12257–12269. https://doi.org/10.1007/s00500-022-07068-x
23. D. Izci, S. Ekinci, C. Budak, V. Gider, PID controller design for DFIG-based wind turbine via reptile search algorithm, In: *2022 Global Energy Conference (GEC)*, 2022, 154–158. https://doi.org/10.1109/GEC55014.2022.9986617
24. M. P. E. Rajamani, R. Rajesh, M. W. Iruthayarajan, Design and experimental validation of PID controller for buck converter: A multi-objective evolutionary algorithms based approach, *IETE J. Res.*, **69** (2023), 21–32. https://doi.org/10.1080/03772063.2021.1905564
25. M. Issa, Enhanced arithmetic optimization algorithm for parameter estimation of PID controller, *Arab J. Sci. Eng.*, **48** (2023), 2191–2205. https://doi.org/10.1007/s13369-022-07136-2
26. Y. Duan, The design of predictive fuzzy-PID controller in temperature control system of electrical heating furnace, In: *Life system modeling and intelligent computing*, Berlin, Heidelberg: Springer, 2010, 259–265. https://doi.org/10.1007/978-3-642-15597-0_29
27. X. Hu, Q. Zou, H. Zou, Design and application of fractional order predictive functional control for industrial heating furnace, *IEEE Access*, **6** (2018), 66565–66575. https://doi.org/10.1109/ACCESS.2018.2878554
28. V. D. Phan, X. H. Nguyen, V. N. Dinh, T. S. Danget, V. C. Le, S. P. Ho, et al., Development of an adaptive fuzzy-neural controller for temperature control in a brick tunnel kiln, *Electronics*, **13** (2024), 342. https://doi.org/10.3390/electronics13020342
29. K. Rsetam, M. AL-Rawi, Z. Cao, Robust state feedback control of electric heating furnace using a new disturbance observer, In: *TENCON 2021-2021 IEEE Region 10 Conference (TENCON)*, 2021, 423–428. https://doi.org/10.1109/TENCON54134.2021.9707435
30. Y. Feng, M. Wu, L. Chen, X. Chen, W. Cao, S. Du, et al., Hybrid intelligent control based on condition identification for combustion process in heating furnace of compact strip production, *IEEE T. Ind. Electron.*, **69** (2022), 2790–2800. https://doi.org/10.1109/TIE.2021.3066918
31. K. Rsetam, M. Al-Rawi, Z. Cao, Robust composite temperature control of electrical tube furnaces by using disturbance observer, *Case Stud. Therm. Eng.*, **30** (2022), 101781. https://doi.org/10.1016/j.csite.2022.101781
32. W. Xu, J. Zhang, R. Zhang, Application of multi-model switching predictive functional control on the temperature system of an electric heating furnace, *ISA T.*, **68** (2017), 287–292. https://doi.org/10.1016/j.isatra.2017.02.001
33. H. Dong, X. Li, X. He, Z. Zeng, G. Wen, A two-degree-of-freedom controller for a high-precision air temperature control system with multiple disturbances, *Case Stud. Therm. Eng.*, **50** (2023), 103442. https://doi.org/10.1016/j.csite.2023.103442
34. Z. Chen, J. Cui, Z. Lei, J. Shen, R. Xiao, Design of an improved implicit generalized predictive controller for temperature control systems, *IEEE Access*, **8** (2020), 13924–13936. https://doi.org/10.1109/ACCESS.2020.2965021
35. D. Izci, S. Ekinci, E. Eker, A. Demirören, Multi-strategy modified INFO algorithm: Performance analysis and application to functional electrical stimulation system. *J. Comput. Sci.*, **64** (2022), 101836. https://doi.org/10.1016/j.jocs.2022.101836

36. T. Veerendar, D. Kumar, CBO-based PID-F controller for Load frequency control of SPV integrated thermal power system, *Mater. Today Proc.*, **58** (2022), 593–599. https://doi.org/10.1016/j.matpr.2022.03.414
37. B. Ozgenc, M. S. Ayas, I. H. Altas, Performance improvement of an AVR system by symbiotic organism search algorithm-based PID-F controller, *Neural Comput. Appl.*, **34** (2022), 7899–7908. https://doi.org/10.1007/s00521-022-06892-4
38. S. Ekinci, H. Çetin, D. Izci, E. Köse, A novel balanced arithmetic optimization algorithm-optimized controller for enhanced voltage regulation, *Mathematics*, **11** (2023), 4810. https://doi.org/10.3390/math11234810
39. D. Izci, R. M. Rizk-Allah, S. Ekinci, A. G. Hussien, Enhancing time-domain performance of vehicle cruise control system by using a multi-strategy improved RUN optimizer, *Alex. Eng. J.*, **80** (2023), 609–622. https://doi.org/10.1016/j.aej.2023.09.009
40. E. Eker, M. Kayri, S. Ekinci, D. Izci, Comparison of swarm-based metaheuristic and gradient descent-based algorithms in artificial neural network training, *ADCAIJ: Adv. Distrib. Comput. Artif. Intell. J.*, **12** (2023), e29969. https://doi.org/10.14201/adcaij.29969
41. R. M. Rizk-Allah, S. Ekinci, D. Izci, An improved artificial rabbits optimization for accurate and efficient infinite impulse response system identification, *Decision Anal. J.*, **9** (2023), 100355. https://doi.org/10.1016/j.dajour.2023.100355
42. W. Zhao, L. Wang, Z. Zhang, H. Fan, Ji. Zhang, S. Mirjalili, et al., Electric eel foraging optimization: A new bio-inspired optimizer for engineering applications, *Expert Syst. Appl.*, **238** (2024), 122200. https://doi.org/10.1016/j.eswa.2023.122200
43. W. Zhou, P. Wang, X. Zhao, H. Chen, Anti-sine-cosine atom search optimization (ASCASO): A novel approach for parameter estimation of PV models, *Environ. Sci. Pollut. Res.*, **30** (2023), 99620–99651. https://doi.org/10.1007/s11356-023-28777-2
44. S. Ekinci, D. Izci, Whale optimization algorithm based controller design for air-fuel ratio system, In: *Handbook of whale optimization algorithm*, Elsevier, 2024, 411–421. https://doi.org/10.1016/B978-0-32-395365-8.00035-X
45. L. Abualigah, A. Diabat, S. Mirjalili, M. Abd Elaziz, A. H. Gandomi, The arithmetic optimization algorithm, *Comput. Methods Appl. Mech. Eng.*, **376** (2021), 113609. https://doi.org/10.1016/j.cma.2020.113609
46. S. Mirjalili, A. Lewis, The whale optimization algorithm, *Adv. Eng. Soft.*, **95** (2016), 51–67. https://doi.org/10.1016/j.advengsoft.2016.01.008
47. A. A. Heidari, S. Mirjalili, H. Faris, I. Aljarah, Harris hawks optimization: Algorithm and applications, *Future Gener. Comp. Syst.*, **97** (2019), 849–872. https://doi.org/10.1016/j.future.2019.02.028
48. E. Rashedi, H. Nezamabadi-pour, S. Saryazdi, GSA: A gravitational search algorithm, *Inform. Sci.*, **179** (2009), 2232–2248. https://doi.org/10.1016/j.ins.2009.03.004
49. M. M. Gani, M. S. Islam, M. A. Ullah, Optimal PID tuning for controlling the temperature of electric furnace by genetic algorithm, *SN Appl. Sci.*, **1** (2019), 880. https://doi.org/10.1007/s42452-019-0929-y
50. V. Sinlapakun, W. Assawinchaichote, Optimized PID controller design for electric furnace temperature systems with Nelder Mead Algorithm, In: *2015 12th International Conference on Electrical Engineering/Electronics, Computer, Telecommunications and Information Technology (ECTI-CON)*, 2015, 1–4. https://doi.org/10.1109/ECTICon.2015.7206925

51. D. A. Bastos, J. Zuanon, L. R. Py-Daniel, C. D.de Santana, Social predation in electric eels, *Ecol. Evol.*, **11** (2021): 1088–1092. https://doi.org/10.1002/ece3.7121
52. G. G. Wang, S. Deb, Z. Cui, Monarch butterfly optimization, *Neural Comput. Appl.*, **31** (2019), 1995–2014. https://doi.org/10.1007/s00521-015-1923-y
53. D. Izci, S. Ekinci, A. Demiroren, J. Hedley, HHO algorithm based PID controller design for aircraft pitch angle control system, In: *2020 International Congress on Human-Computer Interaction, Optimization and Robotic Applications (HORA)*, 2020, 1–6. https://doi.org/10.1109/HORA49412.2020.9152897
54. D. Izci, S. Ekinci, A novel-enhanced metaheuristic algorithm for FOPID-controlled and Bode's ideal transfer function–based buck converter system, *T. I. Meas. Control*, **45** (2023), 1854–1872. https://doi.org/10.1177/01423312221140671
55. Z. L. Gaing, A particle swarm optimization approach for optimum design of PID controller in AVR system, *IEEE T. Energy Conver.*, **19** (2004), 384–391. https://doi.org/10.1109/TEC.2003.821821
56. D. Izci, S. Ekinci, Optimizing three-tank liquid level control: Insights from prairie dog optimization, *Int. J. Robot. Control Syst.*, **3** (2023), 599–608. https://doi.org/10.31763/ijrcs.v3i3.1116
57. M. S. Ali, L. Wang, H. Alquhayz, O. Ur Rehman, G. Chen, Performance improvement of three-phase boost power factor correction rectifier through combined parameters optimization of proportional-integral and repetitive controller, *IEEE Access*, **9** (2021), 58893–58909. https://doi.org/10.1109/ACCESS.2021.3073004
58. E. Çelik, M. Karayel, Effective speed control of brushless DC motor using cascade 1PDf-PI controller tuned by snake optimizer. *Neural Comput. Appl.*, **36** (2024), 7439–7454. https://doi.org/10.1007/s00521-024-09470-y
59. D. Izci, S. Ekinci, An improved RUN optimizer based real PID plus second-order derivative controller design as a novel method to enhance transient response and robustness of an automatic voltage regulator, *e-Prime–Adv. Elect. Eng. Electron. Eng.*, **2** (2022), 100071.

AIMS Press